MICROSTRUCTURE AND REDUCTIBILITY OF TWO MANGANESE ORES AND SINTER PRODUCED FROM THEM[1]

Gisele Buaszczyk[2]
Daniela Marquesini Silva[2]
Anna Zymla[2]
Victor Zymla[2]

Abstract
The purpose of this study has been to better understand the influence of two different manganese ores on structure, mineral composition and reductibility of sinter produced from them. Optical and scanning electronic microscopes as well as X-ray diffraction were used to examine the microstructure and mineral composition of the raw, calcinated and reduced manganese ores as well as the raw and reduced samples of sinter. The coupled TG-FTIR technique was used to simultaneously measure mass losses and evolved gas composition. From the profiles of H_2O and CO_2 measured for each TG test, the temperature ranges of dehydratation, decarbonatation and reduction reactions were identified. The sinter is composed of the manganese oxide grains bonded by a matrix containing smaller grains of manganese oxides surrounded by well crystallized Mn, Fe, Ca silicates and silicoaluminates (formed mainly from ore B) as well as certain amount of K- and Ca-rich silicate glassy phase. The total loss on ignition of ore A and B is 15% and 6% while the total extent of reduction is respectively for ore A, ore B and sinter. The decomposition of higher manganese oxides during calcination and sintering as well as their later reduction to MnO, predicted by the equilibrium calculation, were confirmed by XRD.
Key words: Manganese ores; Sinter; Microstructure; Reductibilty.

ESTRUTURA E REDUCTIBILIDADE DE MINERIOS DE MANGANESES E DO SINTER OBTIDO COM ESSES MINERIOS

Resumo
O objetivo desse estudo foi compreender a influência de dois diferentes de minérios de manganês na estrutura, composição mineralógica e redutibilidade do sínter obtido com esses minérios. Microscopia ótica, MEV e difração de raios-x foram utilizadas para analisar amostras de minério de manganês *in natura*, calcinadas e reduzidas, bem como as amostras de sínter originais e reduzidas. A técnica TG-FTIR foi utilizada para medir simultaneamente as perdas de massa e composição do gás de saída. Através dos perfis de H_2O e CO_2 foram identificados os intervalos de temperatura de desidratação, descarbonatação e reações de redução. O sínter é composto de grãos de óxido de manganês, ligados a matriz que contém pequenos grãos de óxidos de manganês rodeados por cristais bem formados de silicatos de Mn, Fe e Ca e silico-aluminatos e silicatos vítreos ricos em K e Ca. A perda total durante a ignição dos minérios A e B é de 15% e 6%, respectivamente. Essa decomposição durante a calcinação e sinterização, bem como a subseqüente redução de Mn_3O_4 para MnO, prevista pelos cálculos de equilíbrio, foram confirmadas por DRX. A menor taxa de redução de sínter, quando comparado ao minério original, foi finalmente explicada.
Palavras-chave: Mineiro de manganese; Sinter; Estrutura; Redutibilidade.

[1] *Technical contribution to the 3rd International Meeting on Ironmaking, September 22 – 26, 2008, São Luís City – Maranhão State – Brazil*
[2] *École Centrale Paris, France*

1 INTRODUCTION

The reduction of manganese oxides and their ores is being studied with two main aspects in mind. One is a better understanding and optimisation of the reduction and smelting processes which are employed in the production of ferro- and silicomanganese alloys.[1-5] The second reason is more fundamental investigation of oxidation-reduction behaviour of pure manganese oxides, which could be used as active catalysts in several reactions, for example in methane oxidation to produce a syngas or as an oxygen storage component.[6-8]

The ores containing manganese oxides or other minerals rich in manganese used in metallurgical industry, are usually classified according to the country of origin. The mineralogy of main manganese ores deposits in South Africa, Australia, Gabon, Brazil and Ukraine are relatively well known[9,10] but the commercial ore grades change, being continuously adapted to varying demand and supply situation as well as a general technological progress. Sintering is one of the main ways of manganese ore upgrading, used by the most of ore producers. The performance of manganese ore sinter plants as well as a sinter quality depend strongly on the type and quality of ores used for its production[12,13] but even so there is not a lot of studies concerning manganese ores sintering in comparison with the iron ores sintering studies.

The reductibility is one of the most important properties of manganese ore and sinters. It plays a key role in the upper part of the submerged-arc furnace, the main tool for manganese alloys production. In this part of furnace the higher manganese oxides are pre-reduced by carbon monoxide generated in the high temperature melting zone where their reduction process is completed in direct reduction of MnO by carbon. The reductibility of manganese ores and more precisely the kinetics of their reduction was studied by Berg and Olsen[2]. They found that the rate limiting factors for the reduction of higher manganese oxides in manganese ores to divalent manganese oxides depends largely on the mineralogy of the ore. They postulated two different ways of reduction: one for bixbyite/hausmanite rich ore and second for braunite rich ore. In the temperature range of 700 to 1100°C the braunite minerals are more difficult to reduce then bixbyite/hausmanite minerals.

The carbothermic reduction MnO was studied by Ostrovski at al.[3] They found that the reduction rate of MnO in argon-carbon monoxide gas increased with decreasing CO partial pressure. In another study Ostrovski at al.[4] studied the reduction of two different ores: pyrolusite and cryptomelane rich Australian ore and braunit/hausmannite rich South- african ores using CH_4-H_2-Ar gas. They showed that manganese oxides from these ores could be reduced to manganese carbide in the absence of solid carbon. They also found that alkali oxides in Australian ore lower the melting temperature of the ore and thus decrease the reduction rate and extent of reduction at elevated temperatures.

Reduction behaviour of sinter is determined by three factors: chemical composition, pore structure and microstructure (mineralogical composition). These factors interact with each other and are determined by raw material conditions and operational conditions in a sintering process. Mazanek and Wyderko[5-7] studied the process of mineralization in manganese ore sinter. They explained some relationships between the structure and phase composition of sinters and their reductibility and strength.

The purpose of this study has been to characterise individually the behaviour of two different manganese ores in a sintering process and investigate their influence on microstructure and reductibility of the sinter produced from them.

2 MATERIALS AND METHODS

Two manganese ores A and B, as well as a sinter produced from them, were studied. Ore A is a high alumina Brazilian ore and ore B is a high grade South African ore. The thermogravimetric analysis (TGA) of these ores and sinter was performed using a thermobalance (Netzsch TG409) coupled with FTIR spectrometer (Bruker Tensor2), which allow to measure simultaneously the mass losses of sample and the off gas composition (H2O, CO2). Before TGA analysis, the ores were crashed, ground and dried at 100°C.

During the non-isothermal TGA tests with powdered ores and sinter, the sample of about 300 mg and 40-80μm in size was placed in an alumina crucible. It was heated to 1000°C at the heating rate of 20K/min and then maintained at this temperature during 60 min. Nitrogen was used in the calcination treatment and pure carbon monoxide in the reduction treatment. The gas flow rate during both tests was 100 ml/min.

To reduce the influence of mass transfer phenomena on the reduction kinetics at isothermal conditions, thin sinter slabs (10x20x2 mm) were prepared by cutting a sinter lump using a diamond saw. In these TGA tests the samples were heated to the suitable temperature under nitrogen flow at a ramping rate of 20K/min. When the temperature was stabilised, nitrogen was replaced by pure carbon monoxide (at flow rate of 100ml/min).

The morphology and microstructure of raw, calcinated and reduced ores and sinter was examined by optical microscope and by scanning electronic microscope (JEOL T222) with a microanalysis facility (SEM-EDS). To identify mineralogical phases of ores and sinter X-ray diffractometer Siemens D5000 was used.

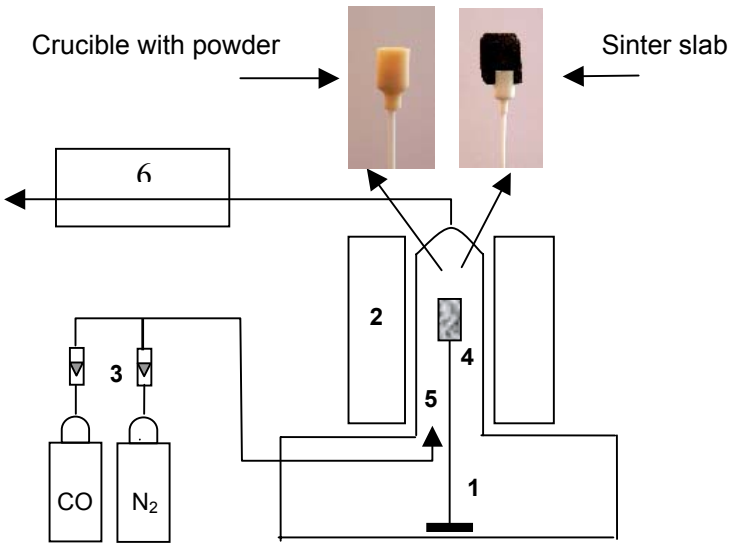

1 - thermobalance, 2 - furnace, 3 - gas flowmeters, 4 - sample on a sample holder (a - crucible with powdered sample, b - crucible with a thin slab), 5 - alumina tube, 6 - gas analyser (FTIR spectrometer)

Figure 1. Experimental set-up used for manganese ore reduction kinetics study.

3 Results

The chemical composition of the ores and sinter under study is given in Table 1.

Table 1. Characteristics of the ores and sinter.

	Mn	Fetot	SiO2	Al2O3	TiO2	CaO	MgO	BaO	K2O	P	lb
Ore A	46.76	4.78	4.21	6.58	0.31	0.22	0.34	0.31	1.83	0.126	0.13
Ore B	48.82	10.37	5.46	0.28	0.06	6.52	0.57	0.58	0.19	0.034	1.30
Sinter	50.91	7.84	6.10	5.81	0.24	5.60	0.11	0.37	1.22	0.088	0.94

A presence of the compounds containing aluminium and potassium in ore A as well as the compounds containing calcium, silicon and iron in ore B was confirmed by local analysis with SEM-EDS (Figure 2).

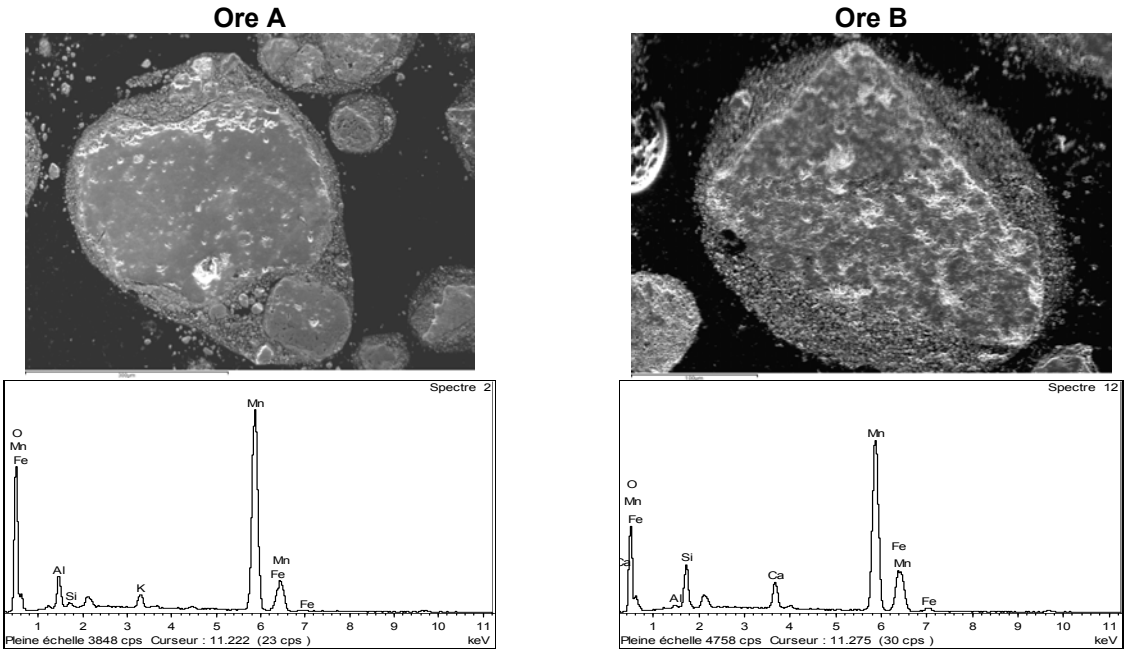

Figure 2. The morphology and elementary composition as seen by SEM-EDS.

From the mineralogical phase analysis by XRD, presented in Figure 3, it can be seen that ore A contains mainly cryptomelane (KMn_8O_{16}), lithiophorite ($LiAl_2Mn,Mn)O_6(OH)_6$, pyrochrosite ($Mn(OH)_2$ and pyrolusite (MnO_2). Ore B is rich in braunite ($CaMn_{14}SiO_{24}$) and also contains manganite ($MnO(OH)$), hematite (Fe_2O_3) and dolomite ($CaMgC_2O_6$).

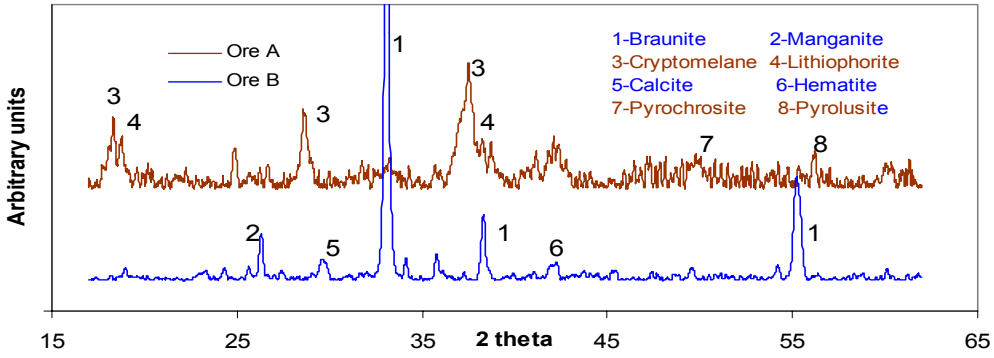

Figure 3. XRD patterns for raw ores A and B.

The results of thermal analysis of two manganese ores are presented in Figures 4 and 5. The mass losses of ore A during the heating in nitrogen up to 1000°C are about 15% while those of ore B are only of 6%. For ore A the mass losses occur at very large temperature range from 100°C to 700°C. They correspond mainly to the dehydration reactions as the presence of water in the evolving gas shows. At higher temperature range, from 700°C to 1000°C the additional 2% of mass loss is measured but with no detectable by FTIR gas release.

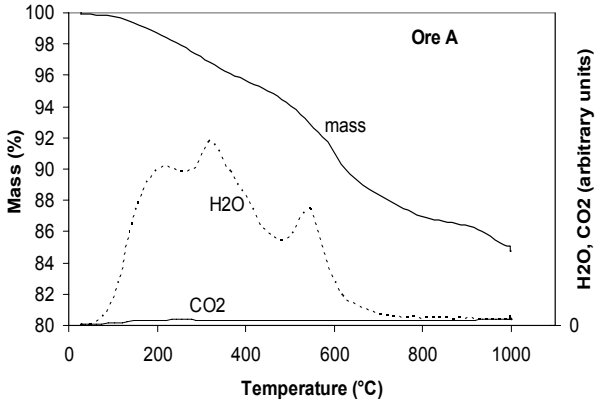

Figure 4. The mass loss and gas composition during the heating of ore A in the nitrogen.

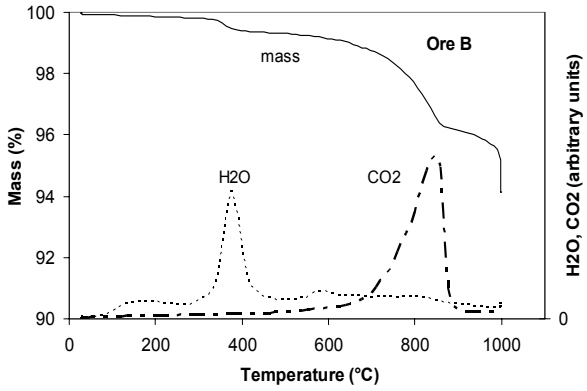

Figure 5. The mass loss and gas composition during the heating of ore B in the nitrogen.

For ore B three successive mass losses occur during heating up to 1000°C. First, very small, of about 1%, is due to the dehydratation at around 400°C. A second, more important, of about 3%, occurs between 700°C and 850°C. It corresponds to the decarbonatation reactions as is shown by the peak of CO_2 detected by FTIR. Between 800°C and 1000°C the mass loss increases of further 2% take place but without gas detectable by FTIR, like during the calcination of ore A.

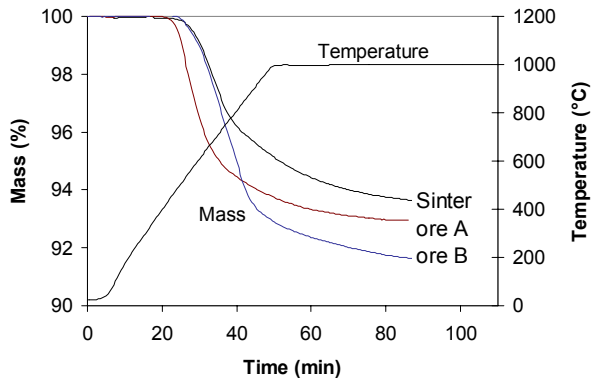

Figure 6. The mass loss evolution during a non-isothermal reduction of the calcinated ores and sinter.

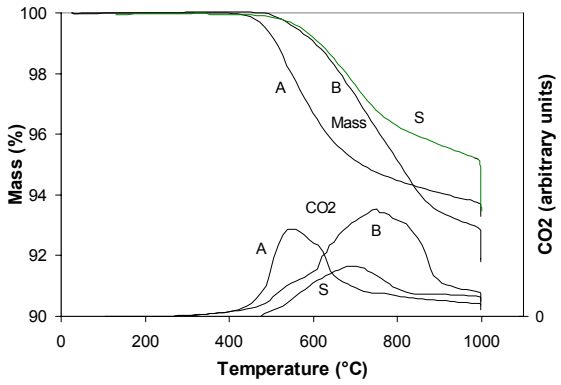

Figure 7. The mass loss and CO_2 evolution during a non-isothermal reduction of the calcinated ores and sinter.

Typical curves obtained during the reduction of powdered calcinated ores and sinter under non-isothermal conditions are presented in Figures 6 and 7. They show that the reduction occurs relatively fast and a bigger part of mass losses is produced during a temperature ramping period. Ore A appears as the most reactive with reduction starting at 450 °C. The reduction of ore B starts later, at around 550°C, but the extent of reduction (8.5%) is greater than that of ore A and sinter, which are respectively 7.5% and 6.5%.

To better understand the mechanism of reduction of sinter, we studied the influence of temperature and sinter particle size on its reduction rate at the isothermal conditions. The effect of temperature on the reduction rate of finely powdered sinter samples (40-80 μm) is shown in Figures 8a and for 2 mm thin slabs in Figure 8b. For both sinter sizes the reduction rate and the final reduction extent increase with temperature. The final mass losses are of around 4%, 6% and 7%, respectively for reduction at 800°C, 900°C and 1000°C.

The effect of particle size on the reduction rate is also illustrated in Figures 8c and 8d. The reduction of finely powdered sinter samples is faster than the reduction of its thin slabs. It can also be seen clearly, especially for a powdered sinter sample, that there are three stages of reduction: first, rather slow with a gradual acceleration; second, very fast and third, very slow when compared with the preceding stages. It should also be noted that the final extent of reduction for slabs and powdered samples is the same for similar reduction conditions.

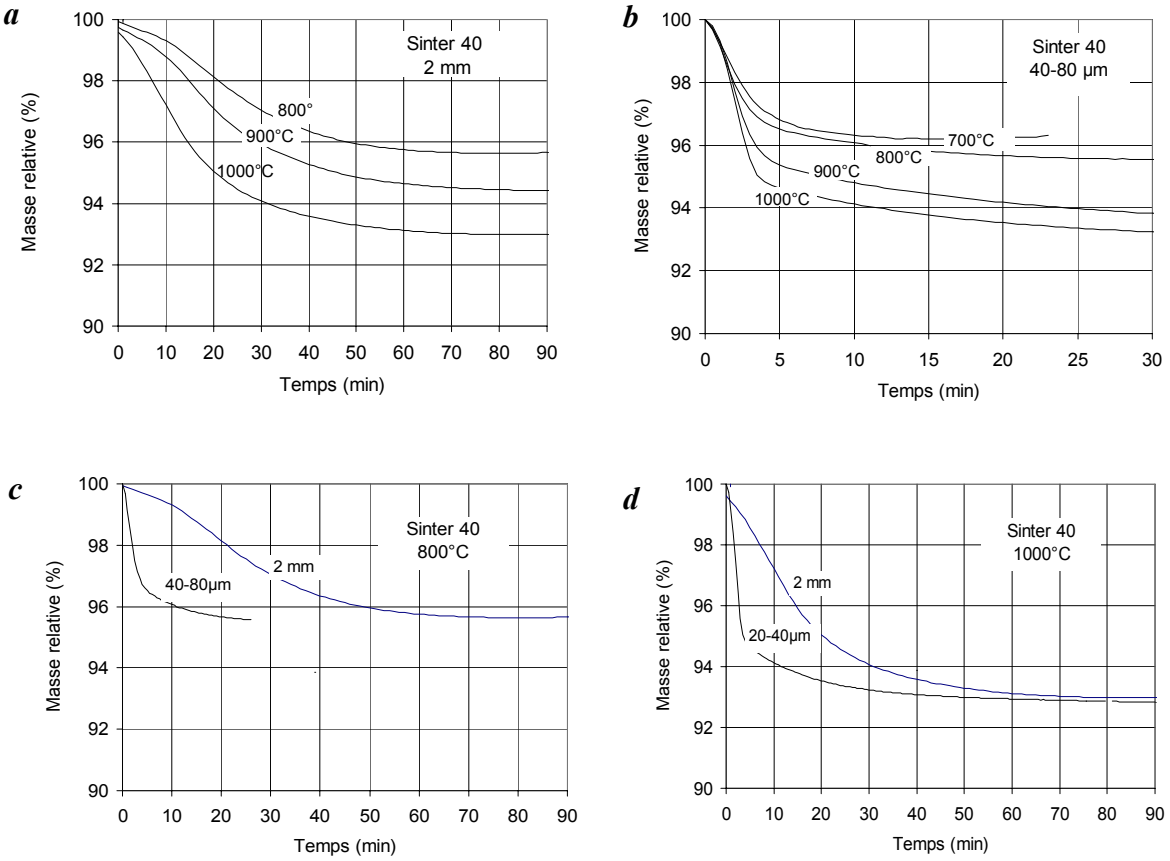

Figure 8. TG curves showing influence of temperature and particles size on kinetics of isothermal reduction of manganese ore sinter in pure CO.

The changes in mineralogical phase composition after calcination and reduction, obtained by XRD analysis, are presented in Figure 9. In both ores two manganese oxides bixbyite (Mn_2O_3) and hausmannite (Mn_3O_4) as well as a jacobsite ($MnFeO_4$) appear after calcination. In reduced ores all higher manganese oxides almost completely disappear except well identified MnO. In ore B, where the iron content is higher than in ore A, the presence of metallic iron was additionally detected.

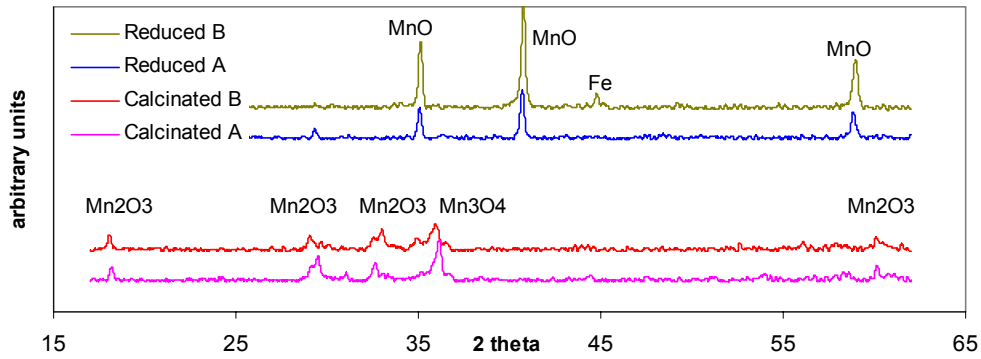

Figure 9. XRD patterns of calcinated and reduced ores A and B

4 DISCUSSION

To better understand the relations between sinter formation and microstructure as well as its reduction kinetics and mechanism, we analysed together the microscopic observations and kinetics data obtained by TG. The microstructure of sinter, presented in Figure 10, shows that it is composed of the fine grains (ranging from few hundred to few microns) having different shapes and sharp edges.

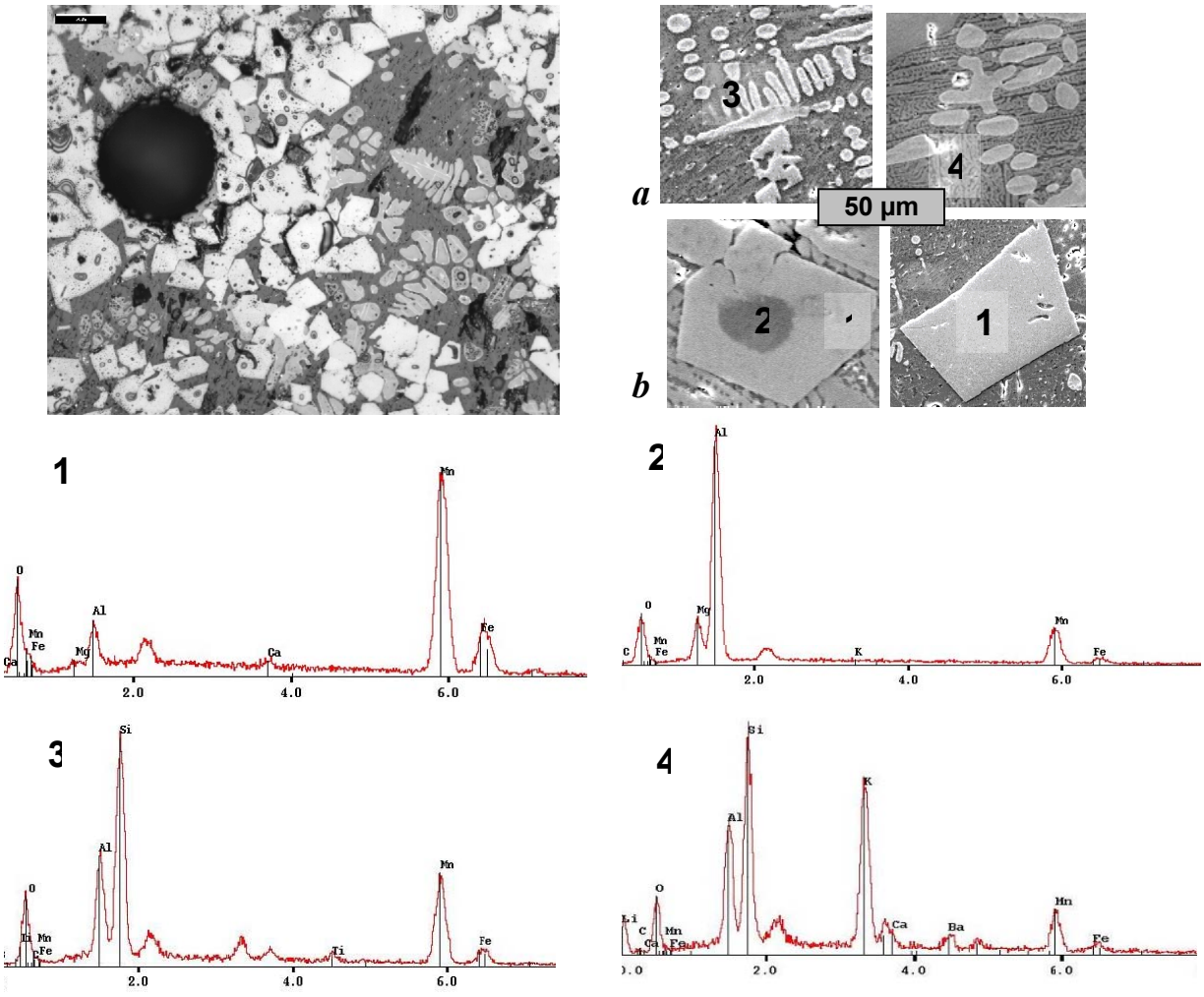

Figure 10. Microstructure of raw manganese ores sinter. a – bonding phase, b – ore grains

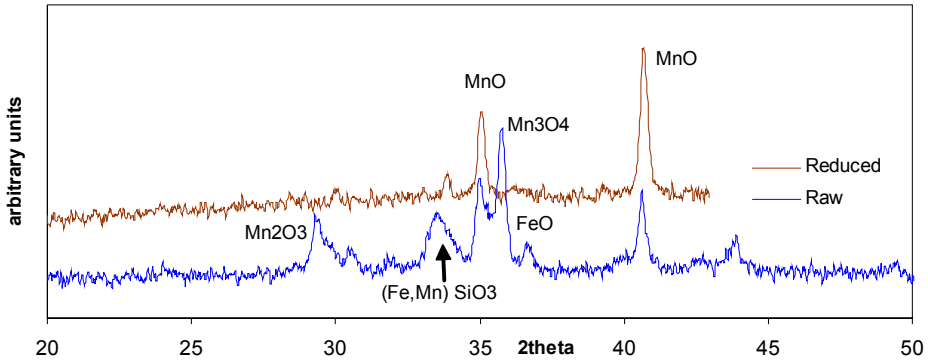

Figure 11. XRD patterns of raw and reduced sinter samples.

They are rich in manganese oxides, but some of them have a core loaded with aluminium. These grains are consolidated by a heterogeneous bonding phase, which contains well crystallized manganese and iron olivines and silico-aluminates surrounded by a glassy phase.

Thus, it could be said that during sinterization, which is more or less an oxidizing process, Mn^{4+} and Mn^{3+} containing phases from ore A are transformed to Mn^{3+} and Mn^{2+} containing oxides (Mn_2O_3, Mn_3O_4 and MnO). At the same time a decomposed braunite type ore B contributes to formation of a liquid phase which after solidification gives some crystallized silicates and silico-aluminates of manganese and iron as well as a glassy phase which concentrates potassium coming from the decomposition of cryptomelane rich ore A.

.

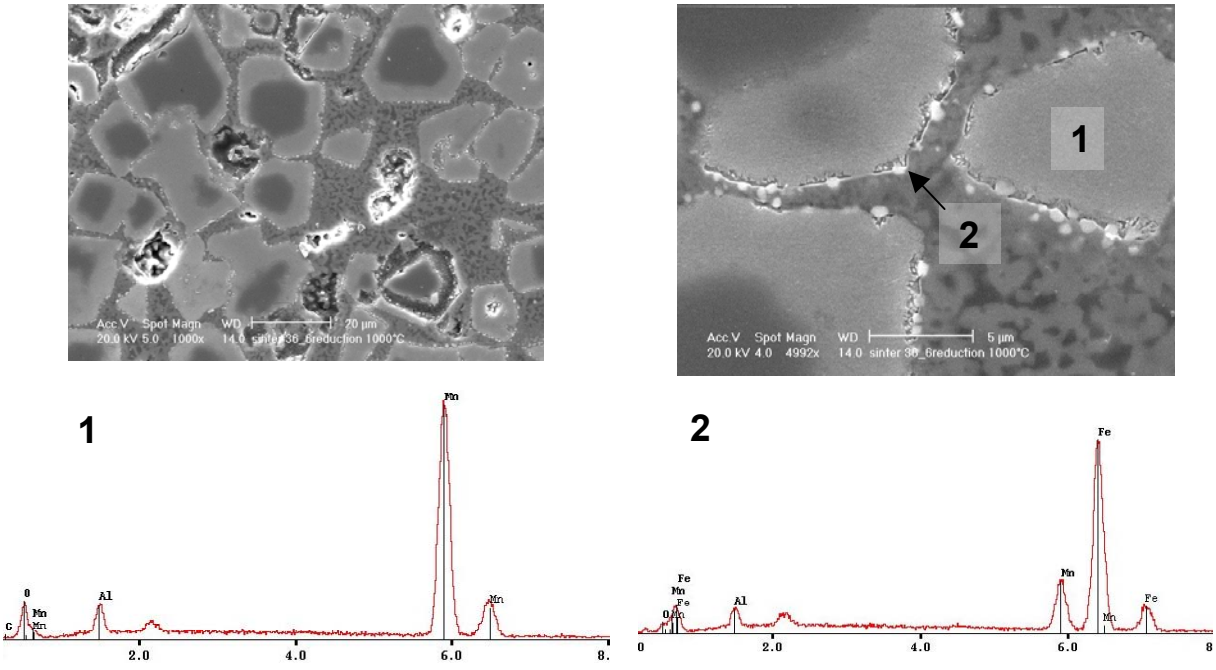

Figure 12. Microstructure of a reduced sinter showing a manganese oxide grains surrounded by metallic iron germs.

The reductibility of sinter depends on these phases content and their spatial distribution. From the XRD analysis and microstructure examination by SEM-EDS it is clear that during the reduction of sinter by carbon monoxide the mass losses are due to the reduction of higher manganese oxides (MnO_2, Mn_2O_3 and Mn_3O_4) to MnO

as well as to the iron oxide reduction to metallic iron. The microphotographs as well as EDS spectra in Figure 12 show the presence of metallic iron germs.

The equilibrium composition calculation of the initial mixture containing 1 mole of Mn_2O_3, 1 mole Mn_3O_4 and 1 mole of $MnOFe_2O_3$ at 1000°C, using HSC Software[14], confirms that the manganese oxides are not stable and even under very low CO concentration (<1%) they could be reduced to MnO (Figure 13a). The iron oxides and mixed manganese-iron oxides (like jarosite) are more stable at this temperature, but in a gas with high CO concentration wustite, unlike MnO, could be completely reduced to metallic iron (Figure 13b).

Taking into account these equilibrium considerations, which obviously only partially explain the observed reduction patterns, it can be said that the reduction starts with manganese and iron higher oxides transformation to MnO and to FeO, respectively (as well as manganowustite MnO*FeO) at almost constant rate but different for different temperatures. After that, reduction of FeO continues more or less slowly according to parabolic kinetics suggesting that diffusion (gaseous or in solid state) plays much more important role.

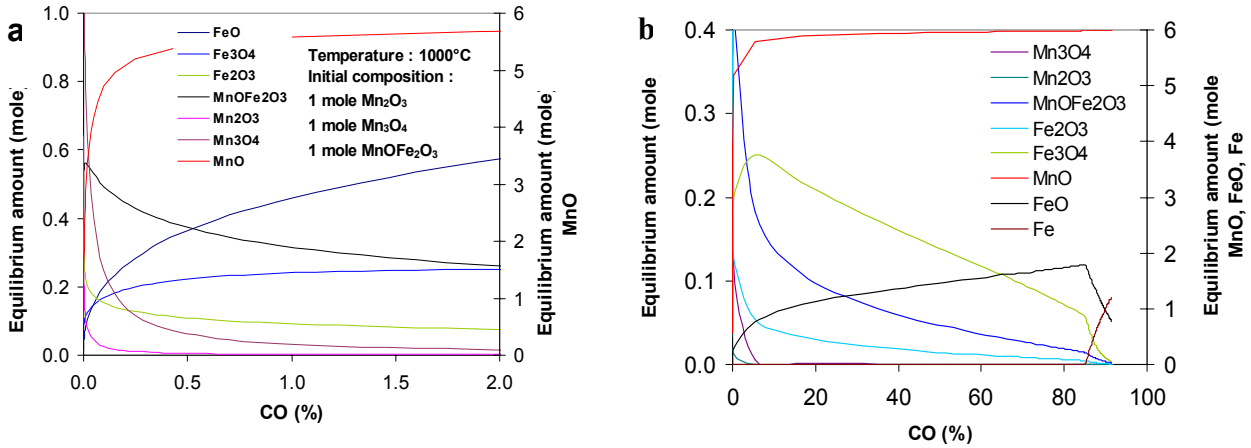

Figure 13. Equilibrium composition of the mixture of manganese and iron oxides at 1000°C (initial composition: 1 mole Mn2O3, 1 mole Mn3O4 and 1 mole MnOFe2O3)

It is also worth to note that in the reduction experiments under isothermal conditions the mass losses (very small <0.2%) were detected under nitrogen flow, when approaching temperature at which nitrogen was replaced by CO as it is shown in Figure 14.

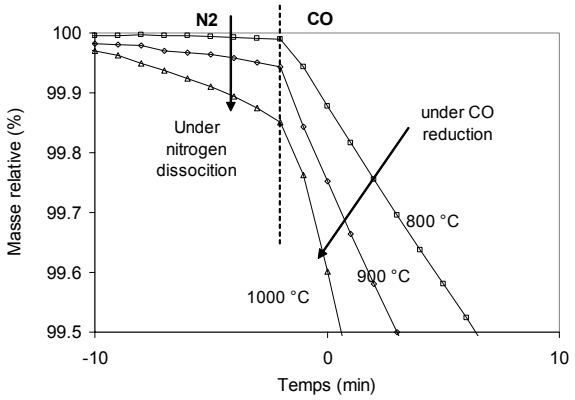

Figure 14. The initial moment of reduction when nitrogen is shifted to carbon monoxide.

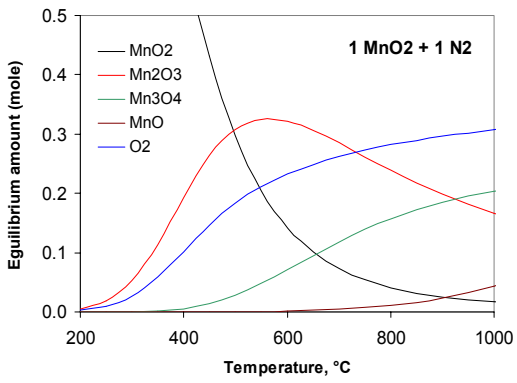

Figure 15. Eguilibrium calculation for 1MnO2+1N2 at 1000°C

The equilibrium calculation, the results of which are presented in Figure 15, confirms the dissociation of MnO_2 when the temperature increases and shows that at 1000°C Mn_2O_3 and Mn_3O_4 could simultaneously occur depending on oxygen partial pressure.

5 CONCLUSIONS

This work was a research project of two Brazilian students coming from UFRGS and UNICAMP and studying at the Ecole Centrale Paris. It provided excellent experience in materials characterisation techniques, such as the optical and electronic microscopy, X-ray diffraction, FTIR spectroscopy and thermal analysis. It was also an occasion to practice the equilibrium calculations using thermo-chemical software in order to predict and understand some of the measured data and observed phenomena.

This study shows that thermal analysis is a very valuable technique for characterisation of manganese ores as well as for sintering and smelting process in an electric furnace. Especially when coupled with a FTIR gas analyser DTA gives a better insight into the reactions occurring during a sintering process, the kinetics of reduction and the total extent of reduction in the upper part of electric furnace. This could be very useful in the assessment of data for a thermal balance of these two main processes of manganese alloys production.

Due to XRD and SEM-EDS analyses it was possible to follow the evolution of complex mineralogical phases mixtures (the manganese ores) to sinter in which the manganese oxides grains originating from cryptomelane rich ore A, were clearly identified. The grains originating from ore B were more difficult to find in the sinter because they were most likely melted and recrystallized as a part of the bonding matrix. Potassium, originally present in ore A, after decomposition of cryptomelane, certainly contributes to the constitution of low temperature melting phase that makes sintering easier. After sinter cooling potassium is found in a glassy part of the bonding matrix.

Acknowledgements

The authors are grateful to Mrs Nathalie Rouscassier from LGPM - ECP for her assistance in SEM-EDS observations and Vale S.A. for providing ores and sinter samples for this student research project.

REFERENCES

1 KOUSARIS A.; FINN C.W.P. The Reduction of Mamatwan Ore in a Submerged-arc Furnace. *Transaction ISIJ*, vol.25, p.109-117, 1987

2 BERG K.L.; OLSEN S.E. Kinetics of Manganese Ore Reduction by Carbon Monoxide. *Met. Trans. B*, vol. 31, p. 477-490, 2000.

3 YASTREBOF, O. OSTROVSKI, S. GANGLY, Effect of Gas Composition on the Carbothermic Reduction of Manganese Oxide. *ISIJ International* vol. 43 p.161-165, 2003

4 O. OSTROVSKI O.; ANACLETO N.; GANGLY S. Reduction of Manganese Ores by Methane-Containing Gas. In: *Proceedings of Tenth International Ferroalloys Congress, INFACON X*, 2004, Cape Town, South Africa. South African Institute of Mining and Metallurgy, p. 173 –183

5 WELHAM N.J. Activation of the carbothermic reduction of manganese ore. *Int. J. Miner. Process*. Vol. 67, p.187-198, 2002
6 STOBBE E.R.; de BOER B.A.; GUES J.W. The reduction and oxidation behaviour of manganese oxides. Catalysis Tooday vol.47 p.161-167, 1999
7 GILLOT B.; El GUENDOUZI M.; LAARJ M. Particle size effects on the oxidation-reduction behavior of Mn3O4 Hausmannite*. Materials Chemistry and Physics* vol70, p.54-60, 2001
8 ZAKI M.I.; HASAN M.A.; PASUPULETY L.; KUMARI K. Thermochemistryof manganese oxides in reactive gas atmospheres: Probing redox composition in the decomposition course MnO2->MnO, *Thermocimica Acta* vol.303 p.171-181, 1997
9 BEAUVAIS A.; MELFI A. ; NAHON D. ; TRESCASES J.J. Pétrologie du gisement latéritique manganésifère d'Azul (Brésil), *Mineral. Deposita* vol. 22 p. 124-134, 1987.
10 J. GUTZMER J.; BEUKES N.J. Mineral paragenesis of Kalahari manganese field, South Africa. *Ore geology Reviews* vol. 11 p. 405-428, 1996.
11 MAZANEK E.; WYDERKO M. Mineralogy and Properties of Iron and Manganese Ore Sinter. *Polska Akademia Nauk, Oddzial W Krakowie, Prace Komisji Metalorgiczno-Odlewniczej, Metalurgia*, n° 22, p 11-14, 1974,
12 TANGSTAD M.; CALVERT P.; BRUN H.; LINDSETH A.G. Use of Comilog Ore in Ferromanganese Production. In: *Proceedings of Tenth International Ferroalloys Congress, INFACON X*, 2004, Cape Town, South Africa. South African Institute of Mining and Metallurgy, p. 213-222.
13 MALAN J.; BARTHEL W.; DIPPENAAR B.A. Optimising Manganese Ore Sinter Plants: Process Parameters and Design Implications. In: *Proceedings of Tenth International Ferroalloys Congress, INFACON X*, 2004, Cape Town, South Africa. South African Institute of Mining and Metallurgy, p. 281-290